

Article

Simulation of Crop Growth and Water-Saving Irrigation Scenarios for Lettuce: A Monsoon-Climate Case Study in Kampong Chhnang, Cambodia

Pinnara Ket ^{1,2,*} , Sarah Garré ³, Chantha Oeurng ¹, Lyda Hok ⁴ and Aurore Degre ² 

¹ Faculty of Hydrology and Water Resources Engineering, Institute of Technology of Cambodia, Russian Federation Bd, P.O. Box 86, Phnom Penh 12156, Cambodia; oeurng_chantha@yahoo.com

² BIOSE, Gembloux Agro-Bio Tech, Liège University, Passage des Déportés 2, Gembloux 5030, Belgium; aurore.degre@uliege.be

³ TERRA, Gembloux Agro-Bio Tech, Liège University, Passage des Déportés 2, Gembloux 5030, Belgium; sarah.garre@uliege.be

⁴ Department of Soil Science, Faculty of Agronomy, Royal University of Agriculture, P.O. Box 2696, Phnom Penh 12401, Cambodia; hoklyda@rua.edu.kh

* Correspondence: ket.pinnara@gmail.com; Tel.: +855-(0)-78-900-477

Received: 19 March 2018; Accepted: 16 May 2018; Published: 21 May 2018



Abstract: Setting up water-saving irrigation strategies is a major challenge farmers face, in order to adapt to climate change and to improve water-use efficiency in crop productions. Currently, the production of vegetables, such as lettuce, poses a greater challenge in managing effective water irrigation, due to their sensitivity to water shortage. Crop growth models, such as AquaCrop, play an important role in exploring and providing effective irrigation strategies under various environmental conditions. The objectives of this study were (i) to parameterise the AquaCrop model for lettuce (*Lactuca sativa* var. *crispa* L.) using data from farmers' fields in Cambodia, and (ii) to assess the impact of two distinct full and deficit irrigation scenarios in silico, using AquaCrop, under two contrasting soil types in the Cambodian climate. Field observations of biomass and canopy cover during the growing season of 2017 were used to adjust the crop growth parameters of the model. The results confirmed the ability of AquaCrop to correctly simulate lettuce growth. The irrigation scenario analysis suggested that deficit irrigation is a “silver bullet” water saving strategy that can save 20–60% of water compared to full irrigation scenarios in the conditions of this study.

Keywords: crop growth; lettuce; AquaCrop; water saving; water productivity; deficit irrigation

1. Introduction

Humanity's environmental footprint is unsustainable within the Earth's limited natural resources and assimilative capacity [1]. Climate change and growth in the global population are increasing pressure on these scarce environmental resources, notably water [2–4]. Particularly, increasing relative evapotranspiration from flow regulation and irrigation over the past century raises the global human water consumption and footprint [5]. Improving food production with less water and benchmarking efficiency of resource use is therefore a great challenge of our time, and urgently needed to ensure food security [1,6,7].

Cambodia is considered to be the country most vulnerable to climate change in Southeast Asia [8]. In recent decades, extreme events, such as floods and droughts, have negatively affected the livelihoods of farmers, especially in terms of the loss of crop production [9]. Cambodian farmers are generally conscious of these changes and challenges [9]. Guidelines for agricultural adaptation to improve crop productivity and the sustainability of the farming system and to minimise vulnerability to

climate change, are therefore crucial [8,10]. Currently, the production of vegetables, like lettuce, poses more challenges in term of managing irrigation water efficiently, due to the crop's sensitivity to water shortage [11–13]. Lettuce, the most widely consumed leaf vegetable, is also one of the most widely cultivated vegetables in the world [14]. It is also an important to local vegetable production in Cambodia [15,16]. Improving strategies for vegetable farming productivity, including lettuce, for Cambodian farmers, is being increasingly considered [17].

Many irrigation strategies have been investigated for improving irrigation water productivity (IWP) during recent decades, with IWP defined as the ratio of agricultural output to the amount of irrigation water use [18]. Full irrigation via water application with the crop evapotranspiration requirements (ET_c) method is an effective irrigation practice for crop production [19–22]. In traditional irrigation scheduling, a technique to meet full irrigation, as well, the soil moisture in the root zone is allowed to fluctuate between an upper limit approximating “field capacity” and the lower limit of the readily accessible water (RAW), referred to as “the threshold”, somewhat above where a crop begins to experience water stress [23,24]. These methods have been applied to improve crop water productivity in various regions of the world, including Asian regions [25–30]. Nevertheless, deficit irrigation, as an adaptation strategy for regions with limited water resources or prone to drought, has been proven to be worth considering [31,32].

Deficit irrigation is an irrigation practice whereby a crop is irrigated with an amount of water below the full requirement for optimal plant growth, thereby saving water and minimising the economic impact on the harvest [18,19]. By limiting water applications to drought-sensitive growth stages such as, the vegetative stages and the late ripening period, the aims of this approach is to maximise water productivity and to stabilise, rather than maximise yields [33]. Water deficit can be defined at five levels: severe deficit (with soil moisture (SM) less than 50% of field capacity (FC)), moderate deficit (SM < 50–60% of FC), mild deficit (SM < 60–70% of FC), no deficit or full irrigation (SM > 70% of FC), and overirrigation (application above water requirements) [34]. Crops under deficit irrigation will experience some level of water stress, and often have lower yields than fully irrigated plants [35]. Deficit irrigation can allow irrigation water savings of up to 20–40% at yield reductions below 10% [36], and has been widely investigated in dry regions [36]. Deficit irrigation can be based on applying irrigation water under crop evapotranspiration. Patanè et al. [37] found that deficit irrigation at 50% of ET_c for tomato plants resulted in no biomass (B) loss and high irrigation water-use efficiency. Experimental results obtained by Abd El-Wahed et al. [38] suggested that deficit irrigation at 85% of ET_c is favourable to save 15% of water provided, with no reduction in the bean crop. The study results of Samperio et al. [39] offered deficit irrigation at 20% and 60% of ET_c during stage II and postharvest, respectively, to “Angeleno” Japanese plum as a water-saving strategy, without negatively affecting crop yield. Results from Yang et al. [40] confirmed that the yield loss for cotton was less than 10% under deficit irrigation of 70% of ET_c and 85% of ET_c. Meanwhile, crop sensitivity to water deficit can be affected by many factors, including climatic conditions, crop species and cultivars, and agronomic management practices, amongst others [34]. Payero et al. [41] suggested that deficit irrigation is not a good strategy for improving the crop water productivity of maize in a semi-arid climate. A study on deficit irrigation treatment on lettuce showed that water stress caused by deficit irrigation at 20% and 40% of ET_c significantly reduced leaf number, leaf area index, and dry matter accumulation [42]. Final fresh weight was reduced by 20% to 30% when compared with full irrigation. Kuslu et al. [43] concluded that for lettuce grown in semi-arid regions, full irrigation should be used under no water shortage, and deficit irrigation by 60% of ET_c could be used for 40% water saving with a 35.8% yield loss where irrigation water supplies are limited.

Elaborating irrigation strategies merely on the basis of field research is difficult and time consuming [44]. Crop models are effective decision-support tools to investigate irrigation scenarios and to develop improved irrigation strategies [7,45,46]. They can provide a rapid and reasonable accurate prediction of the response of agriculture over a range of environmental conditions [47]. The model AquaCrop, developed by the Food and Agricultural Organisation of the United Nations

(FAO), is a water-driven crop model that simulates daily crop growth (e.g., canopy cover and biomass production) and final crop yield, with a balance between accuracy, simplicity, and robustness in incorporating various agronomy practices [48,49]. It is considered as a valuable tool for improving irrigation water productivity in crop production planning [6,50]. AquaCrop has been calibrated and parameterised to various crops under various environmental and irrigation conditions, including barley [51], soybean [52], sunflower [53], cotton [54,55], corn [56], sugar beet [57], wheat [58,59], potato [60,61], cabbage [62], and rice [63]. However, this has not yet been done in the case of lettuce. Most of these studies proved that the model is capable of accurately simulating crop growth and yield. However, some case studies still report some flaws in simulation of crop evolution and yield, especially under severe deficit irrigation and heat stress conditions. Adeboye et al. [64] found that biomass of soybean simulated by AquaCrop was overestimated under deficit irrigation conditions. Zeleke et al. [65] found that AquaCrop simulated the canopy cover and biomass growth of canola well, but the model was less satisfactory under severe water stress conditions in a semi-arid region. Similarly, a reduction in model reliability in biomass and canopy cover prediction for maize under the severe stress conditions of deficit irrigation in a tropical environment was indicated in a study of Greaves et al. [66]. AquaCrop performed well in biomass simulation of potato in the experiment under deficit irrigation at 120, 100, 80, and 60% of ETC [67]. However, the potato yield simulation was overestimated due to the heat stress, with the authors suggesting the incorporation of a temperature stress coefficient into AquaCrop when a crop is affected by high temperatures. Further research is therefore required to improve the performance of AquaCrop. Furthermore, its performance simulating lettuce growth in Cambodian conditions has not yet been tested. The main objective of this study is to improve the water productivity of lettuce under limited irrigations in the Cambodian climate. More specific objectives are (i) to parameterise the crop model AquaCrop using data from farmer fields, since lettuce is not yet available in the AquaCrop catalogue; and (ii) to assess the impact of water-saving scenarios in full and deficit irrigation in silico using this calibrated model.

2. Materials and Methods

2.1. Experimental Sites

The field experiments were conducted with lettuce plants (*Lactuca sativa* var. *crispa* L.) which are widely used in the study area, during a period from August to September 2017 in two experimental sites located in the villages of Chea Rov (site S1) ($104^{\circ}38'54.442''$ E $12^{\circ}9'15.482''$ N) and Ou Rong (site S2) ($104^{\circ}37'16.24''$ E $12^{\circ}11'52.518''$ N) in the province of Kampong Chhnang, Cambodia (Figure 1).

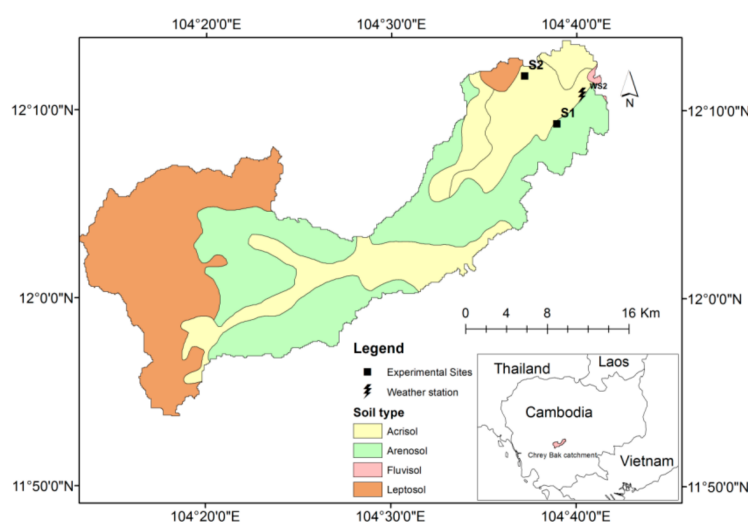


Figure 1. Experimental sites at Chearov (S1) and Ou Rong (S2), located in the Chrey Bak Catchment.

The total land area of the plots was 400 m². Lettuce seeds were sown in standard trays (with 123 holes). After 15 days, seedlings were transplanted into raised bed rows (0.30 m in height and with bed tops 0.50 m wide) and covered with plastic mulch with a planting density of 12 plants m⁻². The compost was basally applied at the rate of 20 ton ha⁻¹ before transplantation.

Irrigation was carried out using a drip system, with emitters of constructor maximum discharge of 3 L h⁻¹ spaced 0.10 m apart. A plastic cover was used to protect the crops from heavy rainfall. Nevertheless, due to the intense rain which flowed between the crop rows, water ponding at 20 cm below the top bed row level was observed between the lettuce rows at both sites during almost the entire growing period. This ponding kept the soil wet during the growing period, and had to be factored into the calibration of the lettuce growing curve. At site S2, irrigation was not applied after a week after planting, due to the benefit of water ponding. At site S1, even though there was also water ponding in the field, the irrigation was applied every other day. The irrigation was determined by checking soil moisture (SM) using the feel and appearance method of Klocke et al. [68]. The irrigation was done when the SM was depleted below field capacity in the root zone at 5 cm, as lettuce have a root depth between 5–10 cm.

2.2. Data Collection and Measurement

2.2.1. Climate Data

Weather data for the experimental sites were collected from a local meteorological station (104°40'21.767" E; 12°10'45.965" N) (Figure 1). Daily maximum and minimum temperature, relative humidity, wind speed, rainfall, and solar radiation were recorded automatically at a five minute time step. The daily reference evapotranspiration (ET_o) for the growing season, used as input data in AquaCrop, was calculated using the ET_o calculator based on the FAO's Penman–Monteith method [69] (Figure 2).

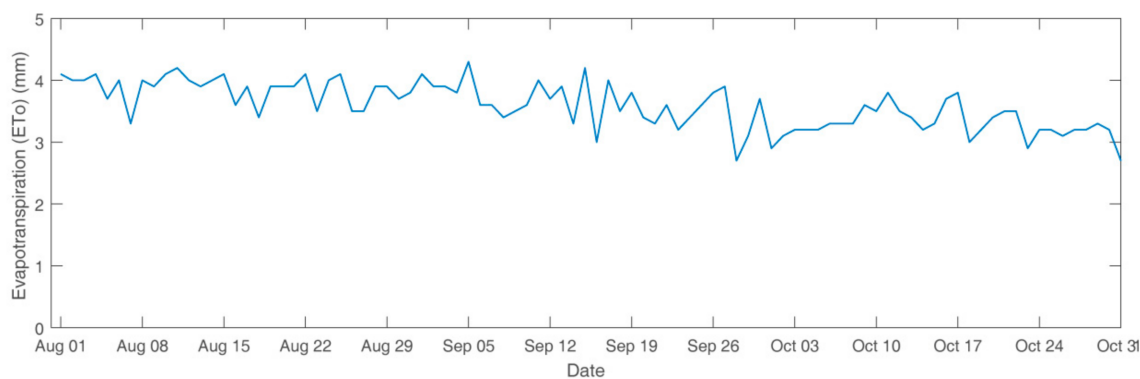


Figure 2. Daily potential evapotranspiration (ET_o) during the growing season 2017.

2.2.2. Soil Data

The physical and chemical soil characteristics which were measured are listed in Tables 1 and 2. The soil texture was measured using the pipette method [70]. The bulk density was measured by the core method [71]. Field capacity, wilting point, and saturated hydraulic conductivity were derived from tension and soil moisture monitoring, using MPS2 and 10HS probes and using inverse modelling as presented in [72].

Table 1. Measured physical soil characteristics.

Parameters	Experimental Sites	
	Chea Rov (S1)	Ou Rong (S2)
Texture	Sand	Loam
Clay (%)	4.39	7.80
Silt (%)	9.56	41.15
Sand (%)	86.03	51.04
Bulk density (g cm ⁻³)	1.5	1.5
Field capacity (m ³ m ⁻³) (sand: at -10 kPa, Loam: at -33 kPa)	0.11	0.14
Wilting point (m ³ m ⁻³) (at 150 kPa)	0.05	0.06
Soil saturation (m ³ m ⁻³)	0.27	0.43
Available water content (AWC) (mm m ⁻¹)	62.48	81.43

Table 2. Measured chemical soil characteristics.

Site	Sampling Time	pH-H ₂ O	EC (uS cm ⁻¹)	OM (%)	N (%)	P (ppm)	K (meg 100 g ⁻¹)	CEC (cmol kg ⁻¹)
S1	Before transplanting	6.28	108	20.31	0.098	13.29	0.77	2.80
	At harvest	6.84	97.4	20.85	0.126	17.08	0.4	4.40
S2	Before transplanting	6.7	223	19.51	0.238	24.07	2.31	7.60
	At harvest	6.8	218	19.78	0.126	15.91	1.45	5.40

Note: EC is electrical conductivity; OM is organic matter content; N is total nitrogen; P is available phosphorous; K is exchangeable potassium; CEC is cation exchange capacity.

2.2.3. Crop Data

Canopy cover was measured at three-day intervals during the growing stage. Four pictures of 1 m² were taken randomly using a digital compact camera (Nikon Coolpix p600, Tokyo, Japan) at a fixed height of 1 m above ground level. The canopy cover was analysed using image processing with ImageJ[®] software (<https://imagej.nih.gov>). Aboveground dry biomass was determined by harvesting 10 heads at the surface level of each site, oven-drying plant samples at 70 °C for 48 h, and weighing them [73].

2.3. AquaCrop Model

The AquaCrop model is a crop water-driven productivity model developed by the FAO in 2009. A detailed description is presented in [49]. Water is the key limiting factor for crop production in this model [74]. Inputs for the AquaCrop model consist of weather data, crop, and soil characteristics (soil profile and groundwater), and field management practice or irrigation management practices [49].

Canopy cover is a crucial feature of AquaCrop [49]. Under unstressed condition, the exponential growth equation to simulate canopy development for the vegetative stage is

$$CC = CC_0 e^{CGC \times t} \quad (1)$$

where CC is the canopy cover at time t and is expressed as fraction of ground covered, CC₀ is initial canopy cover size (at t = 0) as a fraction (%), and CGC is the canopy growth coefficient in fraction per growing degree day (GDD), a constant for a crop under optimal conditions, but modulated by stresses.

In the condition of water stress, the CGC is multiplied by a water stress coefficient of expansive growth (K_{s_{exp}}) (Equation (2)).

$$CGC_{adj} = K_{s_{exp}} \cdot CGC \quad (2)$$

where $K_{s_{exp}}$ ranges from 1 to 0, canopy growth begins to slow down below the maximum rate when soil water depletion reaches the upper threshold, and stops completely when the depletion reaches the lower threshold.

Crop transpiration is proportional to the canopy cover and given by

$$Tr = K_{s_{sto}} K_{C_{Tr}} E_{To} \tag{3}$$

$K_{s_{sto}}$ is the stress coefficient for stomatal closure. $K_{C_{Tr}}$ is the crop transpiration coefficient (determined by canopy cover and $K_{C_{Tr,x}}$), $K_{C_{Tr,x}}$ is the coefficient for maximum crop transpiration, and E_{To} is reference evapotranspiration (mm).

Biomass production is computed from crop transpiration and crop water productivity normalised for E_{To} and CO_2 (Equation (4)). The extreme effect of low temperature on crop phenology, biomass accumulation, and harvest index, is considered with adjustment factors [67,75].

$$B = K_{s_b} \cdot f_{WP} \cdot WP^* \cdot \frac{Tr}{E_{To}} \tag{4}$$

where B is biomass, Tr is crop transpiration ($mm\ day^{-1}$), E_{To} is reference evapotranspiration ($mm\ day^{-1}$), and K_{s_b} is the stress coefficient for low-temperature effects on biomass production. f_{WP} is the adjustment factor to account for differences, if any exist, in the chemical composition of the vegetative biomass and harvestable organs. WP^* is normalised crop water productivity, defined as the ratio of biomass produced to water transpired, normalised for the evaporative demand and CO_2 concentration of the atmosphere.

The AquaCrop stress indicators include water storage (not enough water), waterlogging (too much water), air temperature (too high or too low), and soil salinity stress (too high).

2.4. Model Parameterisation

The process of parameterisation is illustrated in Figure 3. The vegetative stage of lettuce refers to the growing period of lettuce growth after germination until harvest. A growing period during the vegetative stage of 59 days after transplanting was simulated in this study.

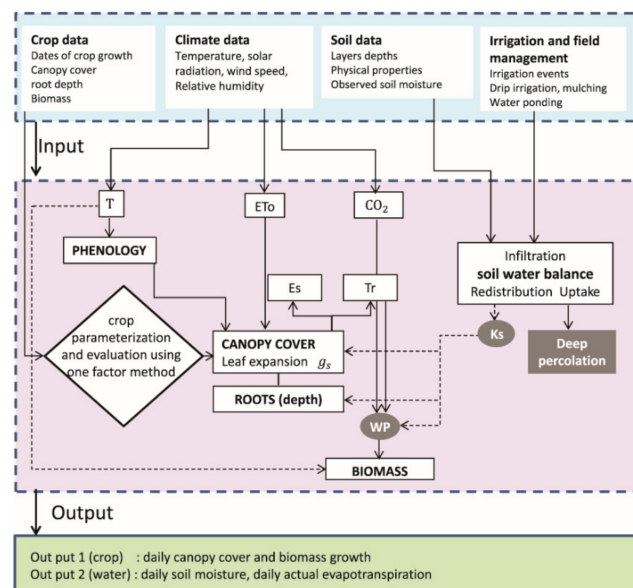


Figure 3. Flow chart of parameterisation of AquaCrop in this study (adjusted from [76]). T is temperature, E_{To} is potential evapotranspiration, g_s is stomatal conductance, WP is water productivity coefficient, K_s is stress coefficient, E_s is soil temperature, Tr is crop transpiration.

As lettuce is a crop which is not yet parameterised in AquaCrop, calibration of the model involved adjusting the model parameters to make them match the observed data [54,77].

The primary variables of lettuce growth, e.g., canopy cover and aboveground biomass were parameterised. For the calibration of the curves, the measured data in two experimental fields at the Chearov site (S1) (having sand soil) and Ourong site (S2) (with loam soil) were used, during the growing season in 2017. The AquaCrop model does not allow the use of observed data to build the canopy cover and biomass curves, but allows the data to be used to calibrate the canopy cover and biomass curves [78].

Canopy cover curves are a plot of the development of leaf expansion response to growing time per day, based on Equation (1). Biomass curves are a relationship plot of the growth of lettuce biomass response to growing time per day, based on Equation (4). The calibration of simulated canopy and biomass curves is based on one-at-a-time (OAT) methods (i.e., changing one parameter at a time while holding others constant) [79] and adjusting the parameters by trial and error, by comparing simulated and observed field data, and minimising the function of root mean square error.

We parameterised the canopy cover curve, which is important to the model for transpiration and evaporation [78]. The main parameters of Equation (1), e.g., CCo and CGC for canopy cover curve determination, were adjusted to match the observed canopy cover data. In addition, adjusting the maximum canopy cover (CCx), time to reach maximum canopy cover, and time to recover, is crucial in order to obtain correct simulations of canopy cover growth. Subsequently, the focus was on adjusting the biomass curve of Equation (4). WP* and $K_{c_{Tr,x}}$ (coefficient for maximum crop transpiration) are the main parameters for regulating biomass curves in AquaCrop [74]. As lettuce is a C3 crop type [80], the recommended values for WP* lie between 15 and 20 g m⁻². All calibrated crop parameters are shown in Table 3.

Table 3. Calibrated parameters of lettuce growth.

No	Calibration Step	Calibrated Parameters
1	Canopy cover calibration	Time to recover of transplant, Time to reach the maximum canopy cover, Initial canopy cover (CCo), Canopy growth coefficient (CGC), Maximum canopy cover growth coefficient (CCx)
2	Biomass calibration	Coefficient for maximum crop transpiration ($K_{c_{Tr,x}}$), Normalised biomass water productivity (WP*)

The model performance for canopy cover and biomass simulation was evaluated using statistic indicators, including root mean square error (RMSE), Nash–Sutcliffe coefficient (N), and coefficient of determination (R^2), defined as below.

$$RMSE = \sqrt{\frac{\sum_{i=1}^n (O_i - S_i)^2}{n}} \quad (5)$$

$$N = 1 - \frac{\sum_{i=1}^n (O_i - S_i)^2}{\sum_{i=1}^n (O_i - \bar{O})^2} \quad (6)$$

$$R^2 = \left(\frac{\sum_{i=1}^n (O_i - \bar{O})(O_i - \bar{S})}{\sqrt{\sum_{i=1}^n (O_i - \bar{O})^2 \sum_{i=1}^n (O_i - \bar{S})^2}} \right)^2 \quad (7)$$

where O and S are the observed and simulated values at time i, respectively, and n is the total amount of the data. When N and R^2 are close to 1, it is considered to be satisfactory [81]. RMSE should be close to 0.

AquaCrop requires the selection of inputs related to the irrigation method, such as sprinkler, drip, or surface. These methods determine the fraction of the soil surface made wet by irrigation [82] and the impact on irrigation efficiency [83].

Default AquaCrop settings for field management include mulching, and use an adjusted factor for the effect of mulches on soil evaporation. It varied between 0.5 for mulches derived from plant material, and 1.0 for plastic mulch [75].

The drip irrigation method with plastic mulch was applied as the input for field management in the model during the parameterisation, as this is the actual practice of the experiment in this study.

The soil water balance calculation, including soil moisture simulation in AquaCrop, is based on the storage capacity of the soil layers, described in Raes et al. [84], and previously in the BUDGET model [85].

During the experimental period, water ponding at 15 cm and 20 cm below the bed soil at site S1 and S2 respectively, which was observed during the experiment, was taken into account as a boundary condition during the parameterisation of the model. This water ponding resulted in wet soil during the growing period. The values of physical soil available data in the Section 2.2.2 were adopted to simulate soil moisture in this study.

It was noted that the plantation experiment was during the rainy season when irrigation was not needed. The crop parameters obtained after parameterisation are important for the investigation of the irrigation scenarios for water saving when irrigation is necessary, especially during the dry season.

2.5. Irrigation Scenarios

In the current study, AquaCrop was used to simulate the full and deficit irrigation scenarios described below (and in Table 4), in order to identify the optimal water use efficiency for lettuce.

Table 4. Irrigation Scenarios.

Scenario Code		Short Description
S1 (Sand)	S2 (Loam)	
Varied readily available water (RAW) threshold irrigation scenarios		
S0RAW	L0RAW	irrigate at 0% of RAW and refill to field capacity (FC)
S50RAW	L50RAW	irrigate at 50% of RAW and refill to FC
S80RAW	L80RAW	irrigate at 80% of RAW and refill to FC
S100RAW	L100RAW	irrigate at 100% of RAW and refill to FC
S120RAW	L120RAW	irrigate at 120% of RAW and refill to FC
S130RAW	L130RAW	irrigate at 130% of RAW and refill to FC
S150RAW	L150RAW	irrigate at 150% of RAW and refill to FC
S180RAW	L180RAW	irrigate at 180% of RAW and refill to FC
S200RAW	L200RAW	irrigate at 200% of RAW and refill to FC
Varied field capacity threshold irrigation scenarios		
S100FC	L100FC	full irrigation-daily irrigation at 100% of field capacity (FC)
S70FC	L70FC	deficit irrigation at 70% of FC
S60FC	L60FC	deficit irrigation at 60% of FC
S50FC	L50FC	deficit irrigation at 50% of FC
S40FC	L40FC	deficit irrigation at 40% of FC

2.5.1. Varied RAW Threshold Irrigation Scenarios

Figure 4 presents the calculation process of varied RAW threshold irrigation scenarios.

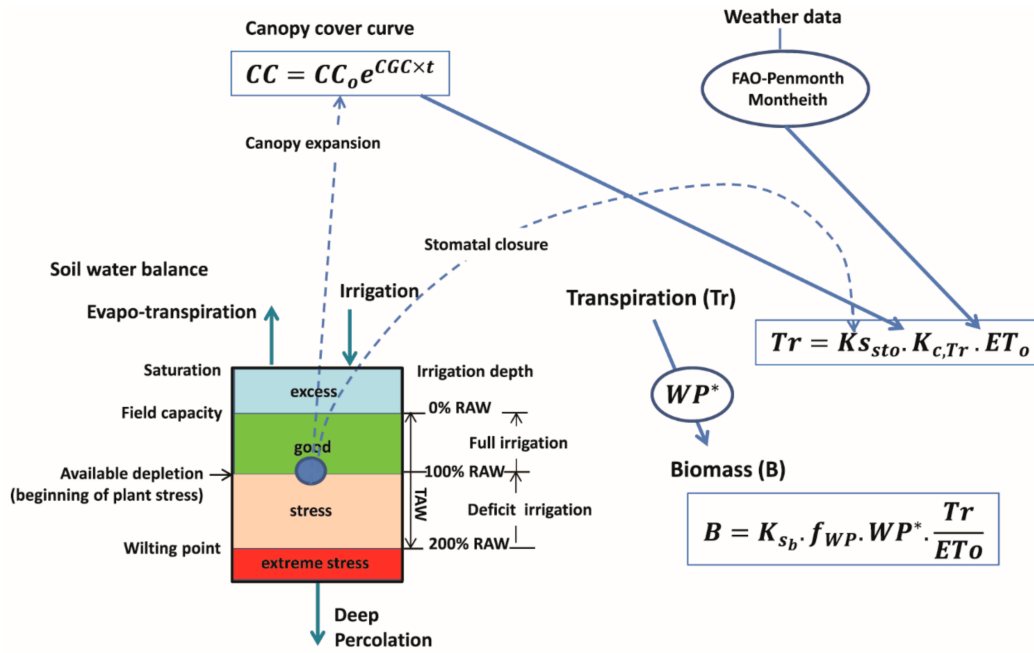


Figure 4. Schematic representation of the crop response to varied RAW threshold irrigation scenarios simulated by AquaCrop (adjusted from [77]). RAW is readily available water content, TAW is total available water content, CC is the simulated canopy cover, CC_o is initial canopy cover size, CGC is canopy growth coefficient in fraction per growing degree day (GDD), $K_{s_{sto}}$ is the water stress for stomatal closure, $K_{c,Tr}$ is the crop transpiration coefficient (determined by CC and $K_{c,Tr,x}$ at maximum canopy cover), ET_o is the reference evapotranspiration, K_{s_b} is the stress coefficient for low-temperature effects on biomass production, f_{WP} is the adjustment factor to account for differences in chemical composition of the vegetative biomass and harvestable organs, WP^* is the normalised water productivity.

These irrigation scenarios applied irrigation scheduling based on soil moisture depletion [86] by applying readily available water depletion in the default option in AquaCrop. The time and irrigation dose were calculated with the criteria below:

1. Soil water content depleted until a fixed lower threshold (RAW) and refill to field capacity (time criteria).
2. Irrigation dose can be determined by the following Equation (8) [87].

$$ID = AD \times RAW \tag{8}$$

where ID is irrigation depth (mm), $RAW = p \ TAW = p \ 1000(FC - PWP)Z_r$, p is soil water depletion threshold, set to 0.3 for lettuce recommended by [69], and Z_r is root depth (m). TAW is the amount of water that a crop can extract from its root zone [88]. FC is field capacity, that is, the amount of water well-drained soil should hold against gravitational forces ($m^3 \ m^{-3}$) [88]. PWP is permanent wilting point, referring to soil water content when a plant fails to recover its turgidity on watering ($m^3 \ m^{-3}$) [88]. RAW is readily available soil water, referring to the fraction of TAW that a crop can extract from the root zone without suffering water stress [88]. AD is allowable depletion, defined as the percentage of RAW that can be depleted before irrigation water has to be applied.

Full irrigation scenarios with varied RAW thresholds were simulated by selecting allowable depletion levels at 0, 50, 80, 100% in AquaCrop, that avoid drought stress during the growth stage [41]. The irrigation schedule is generated by selecting a so-called “time” and “depth” criterion, with “back

to field capacity” and “allowable depletion”, respectively. In other words, the different full irrigation scenarios result in decreasing irrigation frequency.

Deficit irrigation scenarios with varied RAW thresholds were similar to the full irrigation scenario criteria, but applied allowable depletion levels at 120, 130, 150, 180, and 200%. These levels result in drought stress during the growing stage, since soil moisture can decrease to a level below RAW before an irrigation event is triggered [41].

2.5.2. Varied Field Capacity Threshold Irrigation Scenarios

Figure 5 illustrated concept of the varied field capacity threshold irrigation scenarios.

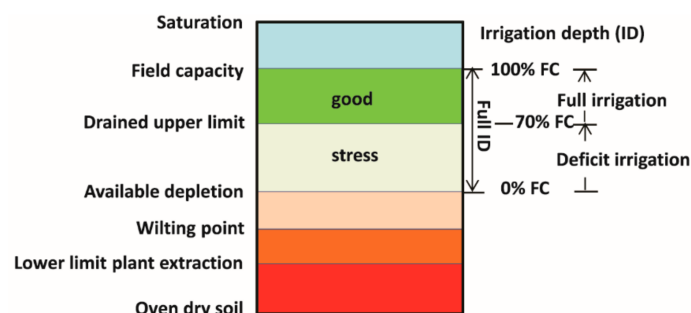


Figure 5. Schematic illustration of the soil water reservoir concepts of varied irrigation depth under field capacity irrigation scenarios (adjusted from [89]). FC is field capacity, full ID is full irrigation depth.

The full irrigation scenario, based on a fixed irrigation frequency maintained the soil moisture in the root zone at field capacity on a daily basis, since the literature claims this is the optimal status to maximise lettuce yield [90]. The irrigation schedule was generated with a fixed time interval (daily) (time criteria) and refill to field capacity (depth criteria).

Deficit irrigation scenarios with varied field capacity threshold reduce the irrigation dose below the dose at field capacity but keeping the same irrigation frequency, as in full irrigation scenario. Daily generated irrigation doses obtained in full irrigation scenario were reduced by 70, 60, 50, and 40%.

Irrigation water productivity (IWP) was used to evaluate the irrigation scenarios for efficient irrigation water use [31,91]. IWP is the ratio between the yield and the irrigation water use [31].

$$IWP = \frac{Y}{I} \quad (9)$$

where IWP is irrigation water productivity (kg m^{-3}), Y is simulated yield (kg ha^{-1}) and interest yield in this study is biomass, and I is irrigation water use (mm).

The adjusted crop parameters obtained from the parameterisation process were used in the scenario simulation under the same weather conditions, using no soil surface cover in model field management, and no ground water at bottom soil profile boundary condition.

3. Results

3.1. Plant Growth and Soil Moisture Status

Figure 6 shows both the lettuce growth measurement and simulation by AquaCrop. Biomass accumulated at a very low rate during the first two weeks of the growing season, and increased sharply in the final week. This trend accords with results obtained by Gallardo et al. [73].

The measured canopy cover and biomass yields were 34% and 0.11 ton ha^{-1} , respectively, at site S1 with sand soil, and 18.5% and 0.11 ton ha^{-1} , respectively, at site S2, which has loam soil. The measured

results are comparable with Fazilah et al. [92], who found observed canopy cover of 33% and biomass yields of 0.22 ton ha⁻¹ for lettuce under similar tropical conditions. Zhang et al. [93] found higher measured biomass for lettuce with a range of 0.33 to 0.63 ton ha⁻¹ under lower temperatures of 20–25 °C. Thus, high day temperatures above 23 °C often limit lettuce production [94]. Optimum growth for lettuce occurs between 15–20 °C [12]. Unfavourable weather conditions, of high average temperature 33/25 °C (day/night) during the experiment, can be the reason of the low measured biomass yields for this study.

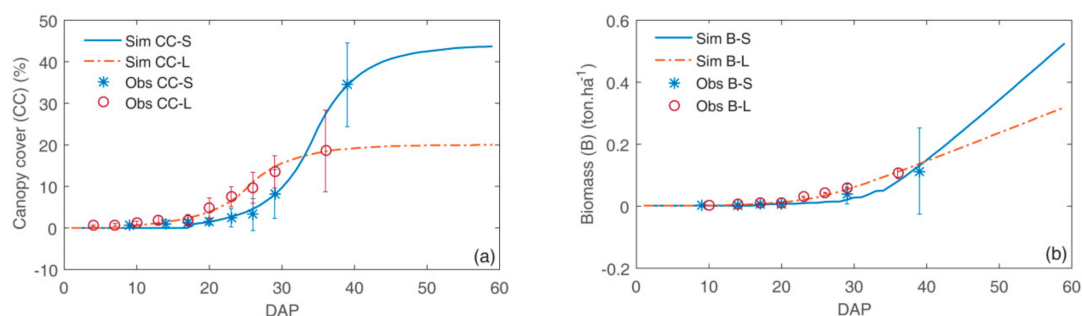


Figure 6. Observed (Obs) data and simulation (Sim) of lettuce growth of AquaCrop: (a) canopy cover at site S1 (CC-S) (sand soil) and site S2 (CC-L) (loam soil); (b) aboveground biomass at site S1 (B-S) and site S2 (B-S). The error bars were based on 10 biomass samples, except the last observed, which was based on 60 samples at harvest time. Sim CC-S is simulated canopy cover at site S1, Sim CC-L is simulated canopy cover at site S2, Obs CC-S is observed canopy cover at site S1, Obs CC-L is observed canopy cover at site S2, Sim B-S is simulated biomass at site S1, Sim B-L is simulated biomass at site S2, Obs B-S is observed biomass at site S1, Obs B-L is observed biomass at site S2.

3.2. Model Parameterisation and Evaluation

The primary crop variables calibrated for daily lettuce growth were canopy cover and biomass, with the daily soil moisture simulated by AquaCrop, by adapting available physical soil data.

Table 5 presents the adjusted model parameters for canopy cover and biomass curve simulation of lettuce growth. The time to recovery of transplant, the time to reach the maximum canopy cover, the initial canopy cover (CCo), the maximum canopy cover growth coefficient (CCx), the coefficient for maximum crop transpiration ($K_{c_{Tr,x}}$), and the normalised biomass water productivity (WP^*) were mainly calibrated.

Table 5. AquaCrop variables parameterised.

Parameters	Symbol and Unit	Value				Sources
		S1		S2		
		Initial	Calibrated	Initial	Calibrated	
Crop Phenology						
Time to recovered transplant (C)	(GDD)	52	280	52	147	Default
Time to maximum canopy cover (C)	(GDD)	563	859	563	727	Default
Crop Growth						
Plant density (NC)	dp (plants m ⁻²)	12	-	12	-	Measure
Initial canopy cover (NC)	CCo (%)	0.72	0.84	0.5	0.6	Default
Maximum effective rooting depth	Zr (m)	0.1	-	0.1	-	Measure
Maximum canopy cover (C)	CCx (%)	34	44	18	20	Measure
Canopy growth coefficient	CGC	22.7	18.5	-	16.8	Default
Base temperature (C)	Tbase (°C)	4	-	4	-	[95]
Upper temperature (C)	Tupper (°C)	28	-	28	-	[96]
Canopy size of transplanted seeding (C)	CC (cm ² plant ⁻¹)	6	-	5	-	Measure
Coefficient for maximum crop transpiration (NC)	$K_{c_{Tr,x}}$	1.25	0.65	1.25	0.5	Default
Water productivity, (C)	WP^* (g m ⁻²)	15	16	15	16	Default

Note: C = conservative, NC = non-conservative.

WP^* was adjusted at 16 gm⁻² for both sites, within the recommended range. $K_{c_{Tr,x}}$ was adjusted at 0.65 and 0.5 for site S1 and S2, respectively. These adjusted $K_{c_{Tr,x}}$ are lower than crop coefficient

for the mid-season ($K_{cb,mid} = 1$) proposed by FAO-56. The difference between the values proposed by FAO-56 and the adjusted $K_{c_{Tr,x}}$ values is due to the fact that the FAO crop coefficients were obtained for specific agroclimatic conditions, which are different from the conditions of this study [78].

In addition, $K_{c_{Tr,x}}$ is a major requisite for estimating crop transpiration and biomass. The low adjusted value of this parameter resulted in low simulated biomass yields to fit to measured values.

High temperature stress observed during the experiment could be the reason for the low observed lettuce biomass production [12]. This observation leads to a recommendation for further development of a heat stress factor in relation to canopy cover and biomass simulations for lettuce.

The minimum root depth cannot be adjusted under 0.1 m, while the root development of lettuce was under this limit. Thus, root development in the model requires further modification [91].

The crop growth simulation of canopy cover and biomass fitted the observed data well (Figure 6). The statistical values for model evaluation in Table 6 were satisfactory, resulting in $R^2 = 0.99$, $RMSE < 0.8\%$, $N < 4.6$ for canopy cover, and $R^2 > 0.98$, $RMSE < 0.01 \text{ ton ha}^{-1}$, $N < -0.07$ for biomass. Thus, the model has ability to simulate well the growth of lettuce in both soil types at the two experimental sites.

Table 6. Statistical evaluation of model simulation.

Statistical Criteria	Sites	Canopy Cover (%)	Biomass (ton ha^{-1})
RMSE	S1	0.69	0.012
	S2	0.84	0.01
R^2	S1	0.99	0.98
	S2	0.99	0.99
N	S1	1.1	-0.015
	S2	4.6	-0.07

The measured and simulated soil moisture, at both soil depths of 5 and 15 cm in both sites, also matched well (Figure 7). The soil moisture simulation resulted in good accuracy with low RMSE of 0.18 and $0.14 \text{ m}^3 \text{ m}^{-3}$ at depths of 5 and 15 cm, respectively, at site S1, and 0.05 and $0.06 \text{ m}^3 \text{ m}^{-3}$ at depths of 5 and 15 cm, respectively, at site S2.

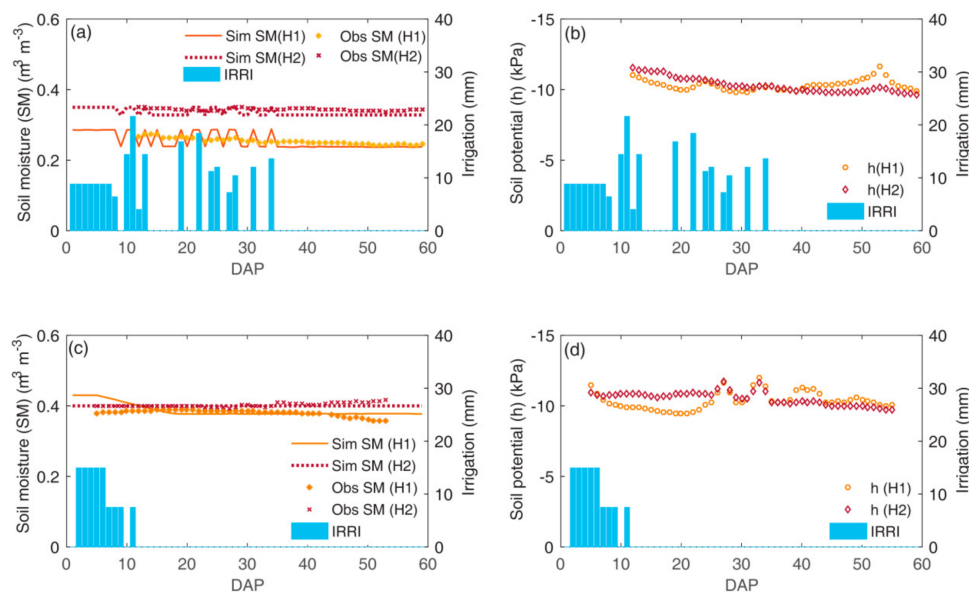


Figure 7. Simulated soil moisture and observed soil moisture data measured at depths of 5 cm (H1) and 15 cm (H2) using soil moisture sensor 10HS and soil potential MPS-2: (a) soil moisture at site S1; (b) soil potential at site S1; (c) soil moisture at site S2; (d) soil potential at site S2. DAP is day after planting, Sim SM is simulated soil moisture, Obs SM is observed soil moisture, IRRi is irrigation, h is soil potential.

3.3. Irrigation Scenarios

3.3.1. Irrigation and Soil Moisture Response

The cumulative irrigation in Figure 8, and the fluctuation of the soil moisture depletion in Figure 9, reflect the interaction between irrigation frequency and amount of water applied.

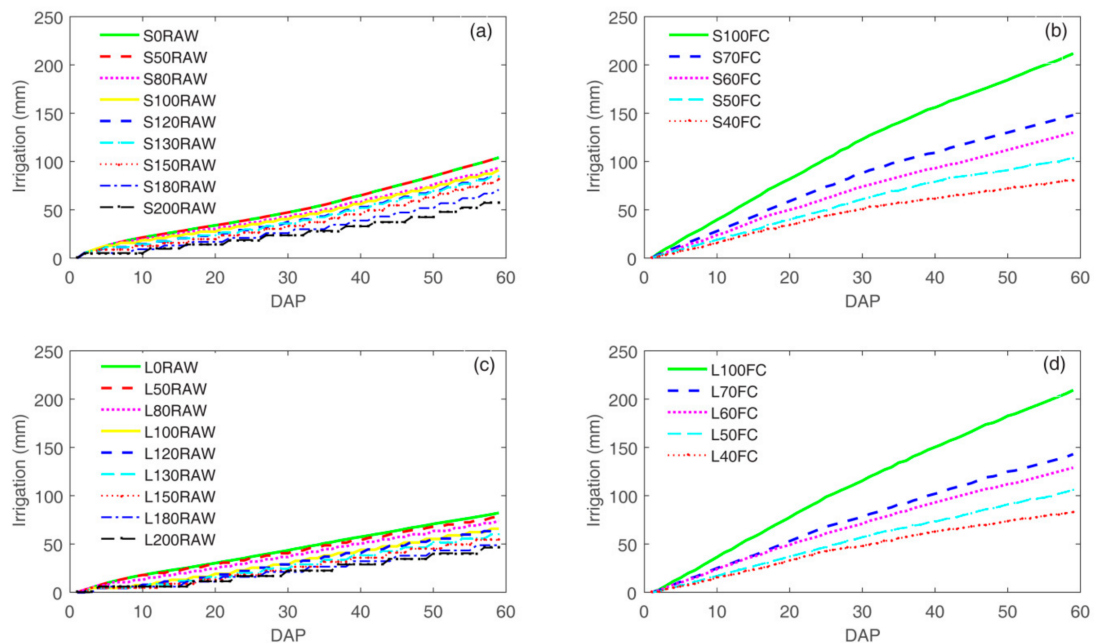


Figure 8. Irrigation accumulation response to different scenarios: (a) varied RAW threshold irrigation scenarios at site S1 (sand soil); (b) varied field capacity threshold irrigation scenarios at site S1; (c) varied RAW threshold irrigation scenarios at site S2 (loam soil); (d) varied field capacity threshold irrigation scenarios at site S2. RAW is readily available water content, S0RAW-S200RAW refers to irrigation scenarios with irrigation at 0–200% of RAW for sand soil. L0RAW-L200RAW refers to irrigation scenarios with irrigation at 0–200% of RAW for loam soil. S40FC-S100FC refers to deficit irrigation at 40–100% of field capacity for sand soil. L40FC-L100FC refers to deficit irrigation at 40–100% of field capacity for loam soil.

In both varied RAW and field capacity threshold irrigation scenarios, the irrigation frequency decreased together with decreasing the amount of water applied per irrigation event.

In varied RAW threshold irrigation scenarios, the simulation of irrigation resulted in irrigation depths which ranged from 57 to 104 mm in site S1 (sand soil) and 46–82 mm in site S2 (loam soil) (Figure 8a,c). In varied field capacity threshold irrigation scenarios, irrigation depths ranged from 81–201 mm in site S1 and 83–209 mm in site S2 (Figure 8b,d).

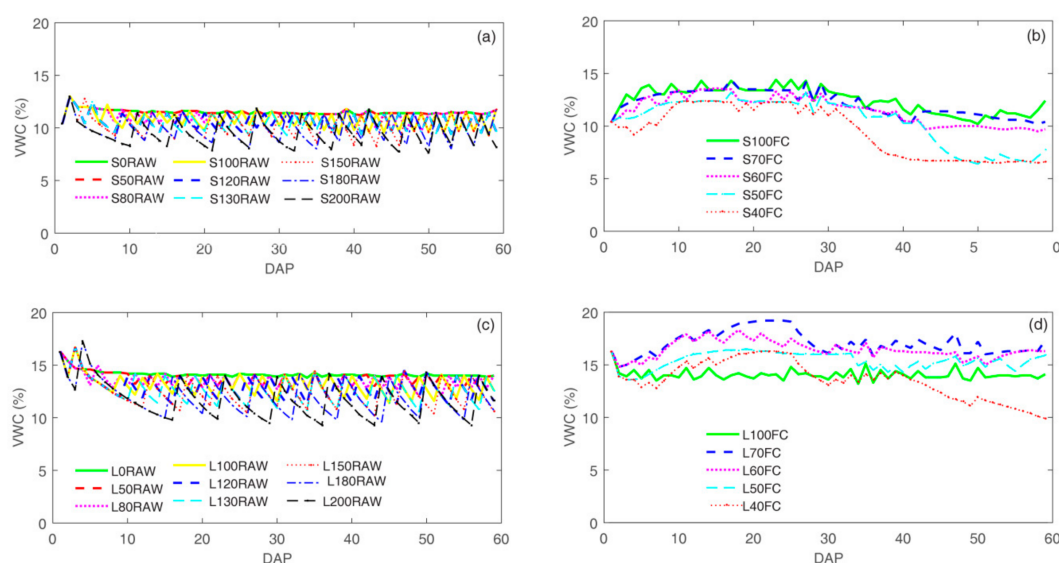


Figure 9. Daily soil moisture (VWC) response to different scenarios: (a) varied RAW threshold irrigation scenarios at site S1 (sand soil); (b) varied field capacity threshold irrigation scenarios at site S1; (c) varied RAW threshold irrigation scenarios at site S2 (loam soil); (d) varied field capacity threshold irrigation scenarios at site S2. RAW is readily available water content, S0RAW-S200RAW refers to irrigation scenarios with irrigation at 0–200% of RAW for sand soil. L0RAW-L200RAW refers to irrigation scenarios with irrigation at 0–200% of RAW for loam soil. S40FC-S100FC refers to deficit irrigation at 40–100% of field capacity for sand soil. L40FC-L100FC refers to deficit irrigation at 40–100% of field capacity for loam soil.

3.3.2. Crop Evapotranspiration and Biomass Growth Response

Figures 10 and 11 illustrate the cumulative crop evapotranspiration (ET_c) and cumulative biomass of lettuce, respectively, under various irrigation scenarios simulated with AquaCrop calibrated for lettuce.

In varied RAW threshold irrigation scenarios, total simulated ET_c ranged from 60 to 100 mm in site S1, and from 53 to 85 mm in site S2 (Figure 10a,c). The main reason for the higher ET_c yield in site S1 is the higher adjusted transpiration characteristic of lettuce in sand soil as compared to loam soil. The simulated values of ET_c fall within the range reported by Abdullah et al. [97] for lettuce, which varied from 43 mm to 285 mm in response to their different irrigation applications between 0 and 267 mm for open surface soil.

In varied field capacity threshold irrigation scenarios, simulated total crop evapotranspiration ranged from 77 to 205 mm in site S1, and from 83 to 211 mm in site S2 (Figure 10b,d). In both irrigation scenario classes, it was noted that while reducing irrigation events, crop evapotranspiration decreased simultaneously.

Figure 11 shows the response of biomass to the different irrigation scenarios. The varied RAW threshold irrigation scenarios (Figure 11a,c) resulted in biomass yield range from 0.88–1.77 ton ha⁻¹ at site S1, and 0.44–0.91 ton ha⁻¹ at site S2. By definition, biomass growth is closely related to crop evapotranspiration. Thus, the difference between biomass yields in the two experimental sites is due to the difference in the K_{cTr,x} (coefficient for maximum crop transpiration) and CC_x (maximum canopy cover) parameters between both sites.

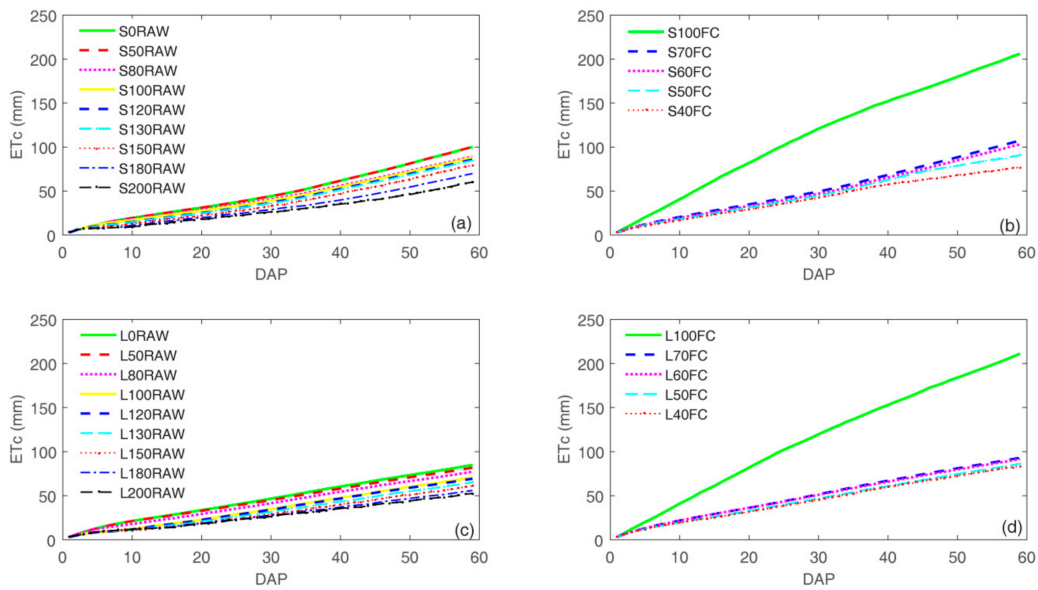


Figure 10. Crop evapotranspiration accumulation responses to different scenarios: (a) varied RAW threshold irrigation scenarios at site S1 (sand soil); (b) varied field capacity threshold irrigation scenarios at site S1; (c) varied RAW threshold irrigation scenarios at site S2 (loam soil); (d) varied field capacity threshold irrigation scenarios at site S2. RAW is readily available water content, S0RAW-S200RAW refers to irrigation scenarios with irrigation at 0–200% of RAW for sand soil. L0RAW-L200RAW refers to irrigation scenarios with irrigation at 0–200% of RAW for loam soil. S40FC-S100FC refers to deficit irrigation at 40–100% of field capacity for sand soil. L40FC-L100FC refers to deficit irrigation at 40–100% of field capacity for loam soil.

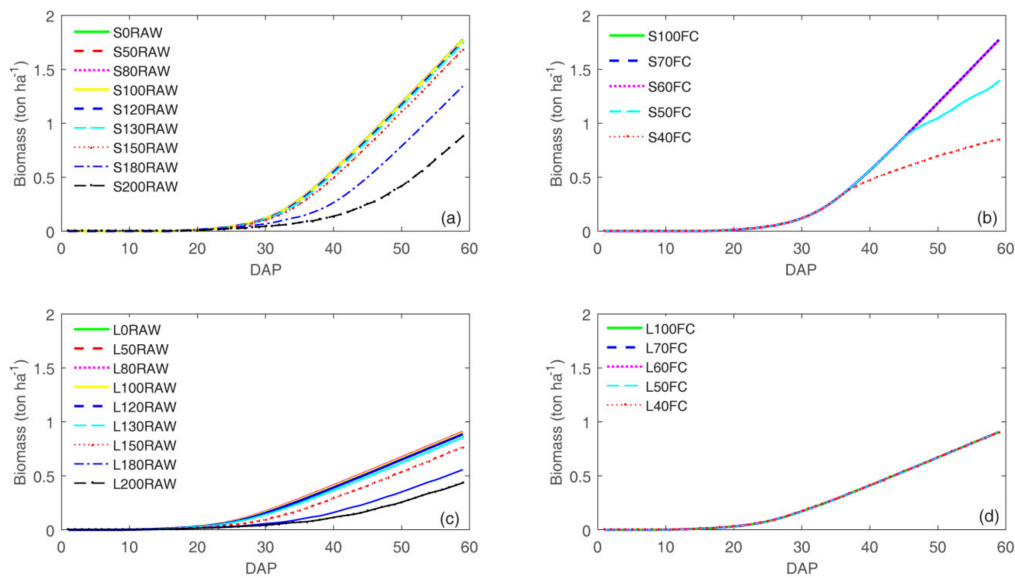


Figure 11. Biomass accumulation responses to different scenarios: (a) varied RAW threshold irrigation scenarios at site S1 (sand soil); (b) varied field capacity threshold irrigation scenarios at site S1; (c) varied RAW threshold irrigation scenarios at site S2 (loam soil); (d) varied field capacity threshold irrigation scenarios at site S2. RAW is readily available water content, S0RAW-S200RAW refers to irrigation scenarios with irrigation at 0–200% of RAW for sand soil. L0RAW-L200RAW refers to irrigation scenarios with irrigation at 0–200% of RAW for loam soil. S40FC-S100FC refers to deficit irrigation at 40–100% of field capacity for sand soil. L40FC-L100FC refers to deficit irrigation at 40–100% of field capacity for loam soil.

As expected, in varied RAW threshold irrigation scenarios, the simulations maintained biomass yield at 1.77 ton ha^{-1} at site S1 and 0.90 ton ha^{-1} at site S2 in the full irrigation scenarios with allowable depletion from 0–100% of RAW (e.g., S0RAW to S100RAW for site S1 and L0RAW to L100RAW for site S2), that is due to no-water stress condition. As the water stress started below the RAW line [41], with available depletion from 120–200% of RAW thresholds, the biomass yields decreased up to 50% in the S200RAW (200% of RAW threshold) scenario at site S1 and 52% in L200RAW scenario at site S2.

In varied field capacity threshold irrigation scenarios (Figure 11b,d), biomass yields ranged from 0.85 to 1.77 ton ha^{-1} at site S1, and 0.89 to 0.90 ton ha^{-1} at site S2. At site S1, reducing deficit irrigation at 50% of field capacity (S50FC scenario), the biomass yield started to decrease with 22% and deficit irrigation at 40% of field capacity (S40FC scenario), biomass yields decreased up to 51% compared to full irrigation scenario (S100FC). For site 2, deficit irrigation up to 40% of field capacity (L40FC) did not affect biomass yield.

3.3.3. Relationship between Water Productivity and Irrigation Scenarios

The responses of biomass yield and irrigation water productivity to irrigation depths in various scenarios are presented in Figure 12. Simulated water productivity of varied RAW threshold irrigation scenarios ranged from 1.5 to 2.1 kg m^{-3} for site S1 and 0.9 to 1.4 kg m^{-3} for site S2. In varied field capacity irrigation scenarios, simulated irrigation water productivity (IWP) ranged from 0.8 to 1.36 kg m^{-3} for site S1 and 0.43– 1.08 kg m^{-3} for site S2. The simulated irrigation water productivity results are comparable with other studies found in the literature. For instance, Gallardo et al. [98] found a measured IWP for lettuce dry matter of 1.86 kg m^{-3} .

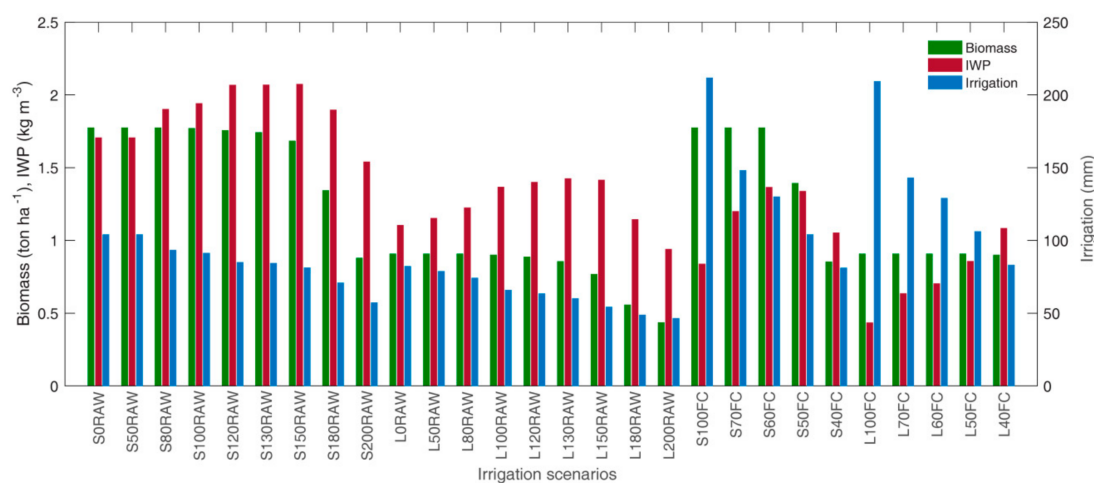


Figure 12. Comparison of biomass and water productivity response (IWP) to different irrigation scenarios. RAW is readily available water content. S0RAW–S200RAW refers to irrigation at 0–200% of RAW threshold irrigation scenarios for sand soil. L0RAW–L200RAW refers to refers to irrigation at 0–200% of RAW threshold irrigation scenarios for loam soil. S40FC–S100FC refers to deficit irrigation at 40–100% of field capacity for sand soil. L40FC–L100FC refers to deficit irrigation at 40–100% of field capacity for loam soil.

Figure 13 shows the relationship curves of biomass yield and irrigation water productivity response to irrigation scenarios. As expected, irrigation water productivity curve response to irrigation depths had parabolic relationships for both soil types in varied RAW threshold irrigation scenarios. Increasing water use efficiency can be enhanced by decreasing the irrigation to an optimum point. The optimum point, which resulted in 22% water saving for site S1, was found at the scenario with depletion of 150% of RAW (S150RAW), resulting in the irrigation water productivity = 2.07 kg m^{-3} , irrigation depth = 81 mm, and biomass yield = 1.68 ton ha^{-1} . For site S2, the optimum irrigation water productivity

was at 130% of RAW scenario (L130RAW), resulting in irrigation water productivity = 1.42 kg m^{-3} , irrigation depth = 60 mm, and biomass yield = 0.85 ton ha^{-1} .

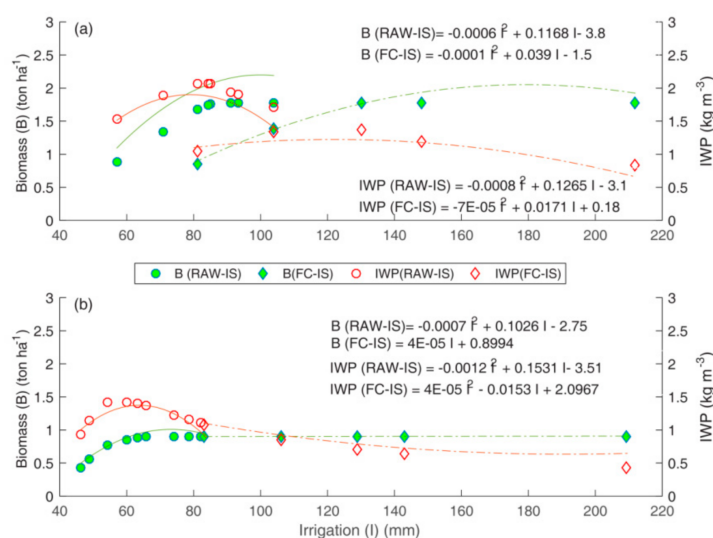


Figure 13. Relationship between biomass and irrigation water productivity responses to different scenarios: (a) at site S1 (sand soil) and (b) at site S2 (loam soil). I is irrigation, B is biomass, IWP is irrigation water productivity, RAW-IS is varied readily available water content threshold irrigation scenarios, FC-IS is varied field capacity threshold irrigation scenarios.

In varied field capacity threshold irrigation scenarios, for site S1, the optimum irrigation water productivity with 39% water saving was found at deficit irrigation at 60% of field capacity (S60FC) with irrigation water productivity = 1.36 kg m^{-3} , irrigation depth = 130 mm, and biomass yield = 1.77 ton ha^{-1} . For site S2, the optimum water productivity resulted in 60% water saving, which was found at deficit irrigation at 40% of field capacity (L40FC scenario) with irrigation water productivity = 1.08 kg m^{-3} , irrigation depth = 83 mm, and biomass yield = 0.89 ton ha^{-1} .

The varied RAW threshold irrigation scenarios resulted in higher simulated higher irrigation water productivity than the varied field capacity threshold scenarios in this study. Overall, deficit irrigation simulation scenarios in both irrigation scenario classes can provide a remarkable improvement in irrigation water productivity for water saving strategies.

3.3.4. Limitation

Crop models, like AquaCrop, are potentially valuable tools for answering questions primarily relating to research understanding, assessing crop management, and policy decision-making [49,99]. However, it is essential to test the models in diverse field environments, such as those with varied temperatures, elevation transects, or amidst latitudinal variations [99]. Particularly, AquaCrop has some limitations in terms of predicting crop yields only at the single growth cycle, single field scale, and only factoring in vertical water balance. The results of this study, obtained using climate data and field observation data relating to lettuce from a single growth cycle experiment at farm scale, allowed important information to be obtained in terms of calibrating lettuce crop parameters for sand and loam soil, and assessing limited water irrigation scenarios in the Cambodian context. However, it remains limited and the uncertainty on parameters has to be kept in mind. This study should be repeated in a contrasting range of diverse environments. Climate conditions and different cultural practices are the variables that differentiate the scenarios between different sites [99,100]. It has been emphasised that uncertainty model simulation results are themselves uncertain, due to known inadequacies of the model (residual errors in measurement) and due to unknown inadequacies of

the model (by inputting new cultivars or different types of management, the model may be wrong in unsuspected ways) [101]. Despite such limitations, AquaCrop has already proven its usefulness in practical applications, and should still be tested widely in broader crop management applications, in diverse field environments [99,100].

4. Conclusions

An AquaCrop model was parameterised to simulate the canopy cover and aboveground biomass growth of lettuce under drip irrigation and plastic mulching for both sand and loam soil in the tropical monsoon climate of Cambodia. The model simulated canopy cover (RMSE < 0.8%) and aboveground biomass (RMSE < 0.01 ton ha⁻¹) in a satisfactory way after adjusting several key parameters, as mentioned in Farahani et al. [54].

Additionally, the results suggested that the incorporation of a heat stress factor affecting canopy cover and biomass growth is necessary to meet the conditions encountered in a tropical climate context.

Shortage of water in Cambodian agriculture has increased due to climate change, and this is a significant challenge facing farmers in their crop production. In this study, the AquaCrop model has helped to develop the simulation process for limited irrigation management strategies to maximise irrigation water productivity. To test the impact of different irrigation scheduling and water saving strategies, two scenario classes were explored: (i) varied readily available water (RAW) threshold irrigation and (ii) varied field capacity threshold irrigation scenarios. The irrigation scenario analysis proposed optimal irrigation strategies for lettuce.

For varied RAW threshold irrigation scenarios, the analysis proposed optimal simulated irrigation water productivity at scenarios of 150% of RAW (irrigation water productivity = 2.1 kg m⁻³) for sand and 130% of RAW (irrigation water productivity = 1.4 kg m⁻³) for loam soil. This can save 22% of water, and resulted in a biomass yield reduction of 5 and 2%, respectively, for sand and loam soil. For varied field capacity threshold irrigation scenarios, the optimal deficit irrigation depth was found at 60% of field capacity (irrigation water productivity of 1.4 kg m⁻³) for sand soil, and at 40% of field capacity (irrigation water productivity of 1.0 kg m⁻³) for loam soil. It can save water up to 39% and 60%, for sand and loam soil, respectively, maintaining biomass yields compared to full irrigation. These results suggest that deficit irrigation is worth considering as a water saving strategy for lettuce in the monsoon climate of Cambodia.

Overall, AquaCrop is a valuable tool to predict lettuce growth and to investigate different scenarios for providing irrigation scheduling strategies for water saving in Cambodia. However, further research is necessary to standardise the model parameters for lettuce in various irrigation management, environmental, and climatic conditions.

Author Contributions: P.K. performed the experiments, analysed the data, and wrote the paper. S.G. advised on the methodologies, gave comments and corrected the manuscript. C.O. supervised the research and gave comments to improve the manuscript. L.H. advised the agronomy practice during the experiments and gave comments on the manuscript. A.D. guided and supervised the research, gave comments, and corrected the manuscript.

Acknowledgments: This study was funded by the Belgian university cooperation programme, ARES-CCD (La Commission Coopération au Développement de l'Académie de Recherche et d'Enseignement supérieur).

Conflicts of Interest: The authors declare no conflict of interest.

References

1. Hoekstra, A.Y.; Wiedmann, T.O. Humanity's Unsustainable Environmental Footprint. *Science* **2014**, *344*, 1114–1117. [[CrossRef](#)] [[PubMed](#)]
2. Bae, J.; Dall'erba, S. Crop Production, Export of Virtual Water and Water-Saving Strategies in Arizona. *Ecol. Econ.* **2018**, *146*, 148–156. [[CrossRef](#)]
3. Rodríguez-Ferrero, N.; Salas-Velasco, M.; Sanchez-Martínez, M.T. Assessment of Productive Efficiency in Irrigated Areas of Andalusia. *Int. J. Water Resour. Dev.* **2010**, *26*, 365–379. [[CrossRef](#)]

4. Chartres, C. Is Water Scarcity a Constraint to Feeding Asia's Growing Population? *Int. J. Water Resour. Dev.* **2014**, *30*, 28–36. [[CrossRef](#)]
5. Jaramillo, F.; Destouni, G. Local Flow Regulation and Irrigation Raise Global Human Water Consumption and Footprint. *Science* **2015**, *350*, 1248–1251. [[CrossRef](#)] [[PubMed](#)]
6. Toumi, J.; Er-Raki, S.; Ezzahar, J.; Khabba, S.; Jarlan, L.; Chehbouni, A. Performance Assessment of AquaCrop Model for Estimating Evapotranspiration, Soil Water Content and Grain Yield of Winter Wheat in Tensift Al Haouz (Morocco): Application to Irrigation Management. *Agric. Water Manag.* **2016**, *163*, 219–235. [[CrossRef](#)]
7. Linker, R.; Ioslovich, I. Assimilation of Canopy Cover and Biomass Measurements in the Crop Model AquaCrop. *Biosyst. Eng.* **2017**, *162*, 57–66. [[CrossRef](#)]
8. Touch, V.; Martin, R.J.; Scott, J.F.; Cowie, A.; Liu, D.L. Climate Change Adaptation Options in Rainfed Upland Cropping Systems in the Wet Tropics: A Case Study of Smallholder Farms in North-West Cambodia. *J. Environ. Manag.* **2016**, *182*, 238–246. [[CrossRef](#)] [[PubMed](#)]
9. Chhinh, N.; Millington, A. Drought Monitoring for Rice Production in Cambodia. *Climate* **2015**, *3*, 792–811. [[CrossRef](#)]
10. Montgomery, S.C.; Martin, R.J.; Guppy, C.; Wright, G.C.; Tighe, M.K. Farmer Knowledge and Perception of Production Constraints in Northwest Cambodia. *J. Rural Stud.* **2017**, *56*, 12–20. [[CrossRef](#)]
11. Moreira, M.A.; Dos Santos, C.A.P.; Lucas, A.A.T.; Bianchini, F.G.; De Souza, I.M.; Viégas, P.R.A. Lettuce Production according to Different Sources of Organic Matter and Soil Cover. *Agric. Sci.* **2014**, *5*, 99–105. [[CrossRef](#)]
12. Valenzuela, H.R.; Bernard, K.; John, C. *Lettuce Production Guidelines for Hawaii*; University of Hawaii: Honolulu, HI, USA, 1996.
13. Cahn, M.; Johnson, L. New Approaches to Irrigation Scheduling of Vegetables. *Horticulturae* **2017**, *3*, 1–20. [[CrossRef](#)]
14. Domingues, D.S.; Takahashi, H.W.; Camara, C.A.P.; Nixdorf, S.L. Automated System Developed to Control pH and Concentration of Nutrient Solution Evaluated in Hydroponic Lettuce Production. *Comput. Electron. Agric.* **2012**, *84*, 53–61. [[CrossRef](#)]
15. Sokhen, C.; Kanika, D.; Moustier, P. *Vegetable Market Flows and Chains in Phnom Penh*; CIRAD-AVRDC-French MOFA: Hanoi, Vietnam, 2004.
16. De Bon, H.; Parrot, L.; Moustier, P. Sustainable Urban Agriculture in Developing Countries. A Review. *Agron. Sustain. Dev.* **2010**, *30*, 21–32. [[CrossRef](#)]
17. Morris, S.; Davies, W.; Baines, R.N. Challenges and Opportunities for Increasing Competitiveness of Vegetable Production in Cambodia. *Acta Hort.* **2013**, *1006*, 253–260. [[CrossRef](#)]
18. Xue, J.; Huo, Z.; Wang, F.; Kang, S.; Huang, G. Untangling the Effects of Shallow Groundwater and Deficit Irrigation on Irrigation Water Productivity in Arid Region: New Conceptual Model. *Sci. Total Environ.* **2018**, *619–620*, 1170–1182. [[CrossRef](#)] [[PubMed](#)]
19. Adu, M.O.; Yawson, D.O.; Armah, F.A.; Asare, P.A.; Frimpong, K.A. Meta-Analysis of Crop Yields of Full, Deficit, and Partial Root-Zone Drying Irrigation. *Agric. Water Manag.* **2018**, *197*, 79–90. [[CrossRef](#)]
20. Liu, Y.; Luo, Y. A Consolidated Evaluation of the FAO-56 Dual Crop Coefficient Approach Using the Lysimeter Data in the North China Plain. *Agric. Water Manag.* **2010**, *97*, 31–40. [[CrossRef](#)]
21. Verstraeten, W.W.; Veroustraete, F.; Feyen, J. Assessment of Evapotranspiration and Soil Moisture Content across Different Scales of Observation. *Sensors* **2008**, *8*, 70–117. [[CrossRef](#)] [[PubMed](#)]
22. Hunsaker, D.J.; French, A.N.; Waller, P.M.; Bautista, E.; Thorp, K.R.; Bronson, K.F.; Andrade-Sanchez, P. Comparison of Traditional and ET-Based Irrigation Scheduling of Surface-Irrigated Cotton in the Arid Southwestern USA. *Agric. Water Manag.* **2015**, *159*, 209–224. [[CrossRef](#)]
23. Thompson, R.B.; Gallardo, M.; Valdez, L.C.; Fernández, M.D. Determination of Lower Limits for Irrigation Management Using in Situ Assessments of Apparent Crop Water Uptake Made with Volumetric Soil Water Content Sensors. *Agric. Water Manag.* **2007**, *92*, 13–28. [[CrossRef](#)]
24. Ferreira, M.I.; Conceição, N.; Malheiro, A.C.; Silvestre, J.M.; Silva, R.M. Water Stress Indicators and Stress Functions to Calculate Soil Water Depletion in Deficit Irrigated Grapevine and Kiwi. *Acta Hort.* **2017**, *1150*, 119–126. [[CrossRef](#)]
25. Li, S.; Kang, S.; Li, F.; Zhang, L. Evapotranspiration and Crop Coefficient of Spring Maize with Plastic Mulch Using Eddy Covariance in Northwest China. *Agric. Water Manag.* **2008**, *95*, 1214–1222. [[CrossRef](#)]

26. Kashyap, P.S.; Panda, R.K. Evaluation of Evapotranspiration Estimation Methods and Development of Crop-Coefficients for Potato Crop in a Sub-Humid Region. *Agric. Water Manag.* **2001**, *50*, 9–25. [[CrossRef](#)]
27. Inthavong, T.; Tsubo, M.; Fukai, S. A Water Balance Model for Characterization of Length of Growing Period and Water Stress Development for Rainfed Lowland Rice. *Field Crop. Res.* **2011**, *121*, 291–301. [[CrossRef](#)]
28. Davis, S.L.; Dukes, M.D. Irrigation Scheduling Performance by Evapotranspiration-Based Controllers. *Agric. Water Manag.* **2010**, *98*, 19–28. [[CrossRef](#)]
29. Kukal, S.S.; Hira, G.S.; Sidhu, A.S. Soil Matric Potential-Based Irrigation Scheduling to Rice (*Oryza sativa*). *Irrig. Sci.* **2005**, *23*, 153–159. [[CrossRef](#)]
30. Pereira, L.S.; Paredes, P.; Sholpankulov, E.D.; Inchenkova, O.P.; Teodoro, P.R.; Horst, M.G. Irrigation Scheduling Strategies for Cotton to Cope with Water Scarcity in the Fergana Valley, Central Asia. *Agric. Water Manag.* **2009**, *96*, 723–735. [[CrossRef](#)]
31. Pereira, L.S.; Cordery, I.; Iacovides, I. Improved Indicators of Water Use Performance and Productivity for Sustainable Water Conservation and Saving. *Agric. Water Manag.* **2012**, *108*, 39–51. [[CrossRef](#)]
32. Afzal, M.; Battilani, A.; Solimando, D.; Ragab, R. Improving Water Resources Management Using Different Irrigation Strategies and Water Qualities: Field and Modelling Study. *Agric. Water Manag.* **2016**, *176*, 40–54. [[CrossRef](#)]
33. Geerts, S.; Raes, D. Deficit Irrigation as an on-Farm Strategy to Maximize Crop Water Productivity in Dry Areas. *Agric. Water Manag.* **2009**, *96*, 1275–1284. [[CrossRef](#)]
34. Chai, Q.; Gan, Y.; Zhao, C.; Xu, H.L.; Waskom, R.M.; Niu, Y.; Siddique, K.H.M. Regulated Deficit Irrigation for Crop Production under Drought Stress. A Review. *Agron. Sustain. Dev.* **2016**, *36*, 1–21. [[CrossRef](#)]
35. Lopez, J.R.; Winter, J.M.; Elliott, J.; Ruane, A.C.; Porter, C.; Hoogenboom, G. Integrating Growth Stage Deficit Irrigation into a Process Based Crop Model. *Agric. For. Meteorol.* **2017**, *243*, 84–92. [[CrossRef](#)]
36. Kögler, F.; Söffker, D. Water (Stress) Models and Deficit Irrigation: System-Theoretical Description and Causality Mapping. *Ecol. Model.* **2017**, *361*, 135–156. [[CrossRef](#)]
37. Patanè, C.; Tringali, S.; Sortino, O. Effects of Deficit Irrigation on Biomass, Yield, Water Productivity and Fruit Quality of Processing Tomato under Semi-Arid Mediterranean Climate Conditions. *Sci. Hortic. (Amsterdam)* **2011**, *129*, 590–596. [[CrossRef](#)]
38. Abd El-Wahed, M.H.; Baker, G.A.; Ali, M.M.; Abd El-Fattah, F.A. Effect of Drip Deficit Irrigation and Soil Mulching on Growth of Common Bean Plant, Water Use Efficiency and Soil Salinity. *Sci. Hortic. (Amsterdam)* **2017**, *225*, 235–242. [[CrossRef](#)]
39. Samperio, A.; Moñino, M.J.; Vivas, A.; Blanco-Cipollone, F.; Martín, A.G.; Prieto, M.H. Effect of Deficit Irrigation during Stage II and Post-Harvest on Tree Water Status, Vegetative Growth, Yield and Economic Assessment in “Angeleno” Japanese Plum. *Agric. Water Manag.* **2015**, *158*, 69–81. [[CrossRef](#)]
40. Yang, C.; Luo, Y.; Sun, L.; Wu, N. Effect of Deficit Irrigation on the Growth, Water Use Characteristics and Yield of Cotton in Arid Northwest China. *Pedosphere* **2015**, *25*, 910–924. [[CrossRef](#)]
41. Payero, J.O.; Melvin, S.R.; Irmak, S.; Tarkalson, D. Yield Response of Corn to Deficit Irrigation in a Semiarid Climate. *Agric. Water Manag.* **2006**, *84*, 101–112. [[CrossRef](#)]
42. Karam, F.; Mounzer, O.; Sarkis, F.; Lahoud, R. Yield and Nitrogen Recovery of Lettuce under Different Irrigation Regimes. *J. Appl. Hortic.* **2002**, *4*, 70–76.
43. Kuslu, Y.; Dursun, A.; Sahin, U.; Kiziloglu, F.M.; Turan, M. Short Communication. Effect of Deficit Irrigation on Curly Lettuce Grown under Semiarid Conditions. *Span. J. Agric. Res.* **2008**, *6*, 714–719. [[CrossRef](#)]
44. Geerts, S.; Raes, D.; Garcia, M. Using AquaCrop to Derive Deficit Irrigation Schedules. *Agric. Water Manag.* **2010**, *98*, 213–216. [[CrossRef](#)]
45. Hassanli, M.; Ebrahimian, H.; Mohammadi, E.; Rahimi, A.; Shokouhi, A. Simulating Maize Yields When Irrigating with Saline Water, Using the AquaCrop, SALTMED, and SWAP Models. *Agric. Water Manag.* **2016**, *176*, 91–99. [[CrossRef](#)]
46. Abderrahman, W.A.; Mohammed, N.; Al-Harazin, I.M. Computerized and Dynamic Model for Irrigation Water Management of Large Irrigation Schemes in Saudi Arabia. *Int. J. Water Resour. Dev.* **2001**, *17*, 261–270. [[CrossRef](#)]
47. Wolf, J.; Evans, L.G.; Semenov, M.A.; Eckersten, H.; Iglesias, A. Comparison of Wheat Simulation Models under Climate Change. I. Model Calibration and Sensitivity Analyses. *Clim. Res.* **1996**, *7*, 253–270. [[CrossRef](#)]

48. Ran, H.; Kang, S.; Li, F.; Tong, L.; Ding, R.; Du, T.; Li, S.; Zhang, X. Performance of AquaCrop and SIMDualKc Models in Evapotranspiration Partitioning on Full and Deficit Irrigated Maize for Seed Production under Plastic Film-Mulch in an Arid Region of China. *Agric. Syst.* **2017**, *151*, 20–32. [[CrossRef](#)]
49. Steduto, P.; Hsiao, T.C.; Raes, D.; Fereres, E. AquaCrop—The FAO Crop Model to Simulate Yield Response to Water: I. Concepts and Underlying Principles. *Agron. J.* **2009**, *101*, 426–437. [[CrossRef](#)]
50. Singh, A.; Saha, S.; Mondal, S. Modelling Irrigated Wheat Production Using the FAO AquaCrop Model in West Bengal, India, for Sustainable Agriculture. *Irrig. Drain.* **2013**, *62*, 50–56. [[CrossRef](#)]
51. Tavakoli, A.R.; Mahdavi Moghadam, M.; Sepaskhah, A.R. Evaluation of the AquaCrop Model for Barley Production under Deficit Irrigation and Rainfed Condition in Iran. *Agric. Water Manag.* **2015**, *161*, 136–146. [[CrossRef](#)]
52. Paredes, P.; Wei, Z.; Liu, Y.; Xu, D.; Xin, Y.; Zhang, B.; Pereira, L.S. Performance Assessment of the FAO AquaCrop Model for Soil Water, Soil Evaporation, Biomass and Yield of Soybeans in North China Plain. *Agric. Water Manag.* **2015**, *152*, 57–71. [[CrossRef](#)]
53. Todorovic, M.; Albrizio, R.; Zivotic, L.; Saab, M.-T.A.; Stöckle, C.; Steduto, P. Assessment of AquaCrop, CropSyst, and WOFOST Models in the Simulation of Sunflower Growth under Different Water Regimes. *Agron. J.* **2009**, *101*, 509–521. [[CrossRef](#)]
54. Farahani, H.J.; Izz, G.; Oweis, T.Y. Parameterization and Evaluation of the AquaCrop Model for Full and Deficit Irrigated Cotton. *Agron. J.* **2009**, *101*, 469–476. [[CrossRef](#)]
55. Hussein, F.; Janat, M.; Yakoub, A. Simulating Cotton Yield Response to Deficit Irrigation with the FAO AquaCrop Model. *Span. J. Agric. Res.* **2011**, *9*, 1319–1330. [[CrossRef](#)]
56. Hsiao, T.C.; Heng, L.; Steduto, P.; Rojas-Lara, B.; Raes, D.; Fereres, E. AquaCrop—The FAO Crop Model to Simulate Yield Response to Water: III. Parameterization and Testing for Maize. *Agron. J.* **2009**, *101*, 448–459. [[CrossRef](#)]
57. Malik, A.; Shakir, A.S.; Ajmal, M.; Khan, M.J.; Khan, T.A. Assessment of AquaCrop Model in Simulating Sugar Beet Canopy Cover, Biomass and Root Yield under Different Irrigation and Field Management Practices in Semi-Arid Regions of Pakistan. *Water Resour. Manag.* **2017**, *31*, 4275–4292. [[CrossRef](#)]
58. Andarzian, B.; Bannayan, M.; Steduto, P.; Mazraeh, H.; Barati, M.E.; Barati, M.A.; Rahnama, A. Validation and Testing of the AquaCrop Model under Full and Deficit Irrigated Wheat Production in Iran. *Agric. Water Manag.* **2011**, *100*, 1–8. [[CrossRef](#)]
59. Mkhabela, M.S.; Bullock, P.R. Performance of the FAO AquaCrop Model for Wheat Grain Yield and Soil Moisture Simulation in Western Canada. *Agric. Water Manag.* **2012**, *110*, 16–24. [[CrossRef](#)]
60. Rankine, D.R.; Cohen, J.E.; Taylor, M.A.; Coy, A.D.; Simpson, L.A.; Stephenson, T.; Lawrence, J.L. Parameterizing the FAO AquaCrop Model for Rainfed and Irrigated Field-Grown Sweet Potato. *Agron. J.* **2015**, *107*, 375–387. [[CrossRef](#)]
61. Casa, A. De; Ovando, G.; Bressanini, L.; Martínez, J. Aquacrop Model Calibration in Potato and Its Use to Estimate Yield Variability under Field Conditions. *Atmos. Clim. Sci.* **2013**, *3*, 397–407. [[CrossRef](#)]
62. Wellens, J.; Raes, D.; Traore, F.; Denis, A.; Djaby, B.; Tychon, B. Performance Assessment of the FAO AquaCrop Model for Irrigated Cabbage on Farmer Plots in a Semi-Arid Environment. *Agric. Water Manag.* **2013**, *127*, 40–47. [[CrossRef](#)]
63. Deb, P.; Tran, D.A.; Udmale, P.D. Assessment of the Impacts of Climate Change and Brackish Irrigation Water on Rice Productivity and Evaluation of Adaptation Measures in Ca Mau Province, Vietnam. *Theor. Appl. Climatol.* **2016**, *125*, 641–656. [[CrossRef](#)]
64. Adeboye, O.B.; Schultz, B.; Adekalu, K.O.; Prasad, K. Modelling of Response of the Growth and Yield of Soybean to Full and Deficit Irrigation by Using Aquacrop. *Irrig. Drain.* **2017**, *66*, 192–205. [[CrossRef](#)]
65. Zeleke, K.T.; Lockett, D.; Cowley, R. Calibration and Testing of the FAO AquaCrop Model for Canola. *Agron. J.* **2011**, *103*, 1610–1618. [[CrossRef](#)]
66. Greaves, G.E.; Wang, Y.M. Assessment of Fao Aquacrop Model for Simulating Maize Growth and Productivity under Deficit Irrigation in a Tropical Environment. *Water* **2016**, *8*, 1–18. [[CrossRef](#)]
67. Montoya, F.; Camargo, D.; Ortega, J.F.; Córcoles, J.I.; Domínguez, A. Evaluation of Aquacrop Model for a Potato Crop under Different Irrigation Conditions. *Agric. Water Manag.* **2016**, *164*, 267–280. [[CrossRef](#)]
68. Klocke, N.L.; Fischbach, P.E. G84-690 Estimating Soil Moisture by Appearance and Feel. In *Historical Materials from University of Nebraska-Lincoln Extension*; University of Nebraska: Lincoln, NE, USA, 1984; pp. 1–9.

69. Allen, R.G.; Pereira, L.S.; Raes, D.; Smith, M. Crop Evapotranspiration: Guidelines for Computing Crop Water Requirements. *Irrig. Drain.* **1998**, *300*, 300.
70. Pansu, M.; Gautheyrou, J. *Handbook of Soil Analysis: Mineralogical, Organic and Inorganic Methods*; Springer Science & Business Media: Berlin, Germany, 2007.
71. Margesin, R.; Schinner, F. *Manual for Soil Analysis-Monitoring and Assessing Soil Bioremediation*; Springer Science & Business Media: Berlin, Germany, 2005.
72. Ket, P.; Garré, S.; Oeurng, C.; Degré, A. *A Comparison of Soil Water Retention Curves Obtained Using Field, Lab and Modelling Methods in Monsoon Context of Cambodia*; ARES-CCD: Brussels, Belgium, 2018.
73. Gallardo, M.; Jackson, L.E.E.; Schulbach, K.; Snyder, R.L.L.; Thompson, R.B.B.; Wyland, L.J.J. Production and Water Use in Lettuces under Variable Water Supply. *Irrig. Sci.* **1996**, *16*, 125–137. [[CrossRef](#)]
74. Razzaghi, F.; Zho, Z.; Andersen, M.; Plauborg, F. Simulation of Potato Yield in Temperate Condition by the AquaCrop Model. *Agric. Water Manag.* **2017**, *191*, 113–123. [[CrossRef](#)]
75. Raes, D.; Steduto, P.; Hsiao, T.C.; Fereres, E. AquaCrop—The FAO Crop Model to Simulate Yield Response to Water: II. Main Algorithms and Software Description. *Agron. J.* **2009**, *101*, 438–447. [[CrossRef](#)]
76. Steduto, P.; Raes, D.; Hsiao, T.; Fereres, E. AquaCrop: A New Model for Crop Prediction under Water Deficit Conditions. *Options Méditerr.* **2009**, *33*, 285–292.
77. Steduto, P.; Hsiao, T.C.; Fereres, E.; Raes, D. *Crop Yield Response to Water*; The Food and Agriculture Organization (FAO): Rome, Italy, 2012.
78. Paredes, P.; de Melo-Abreu, J.P.; Alves, I.; Pereira, L.S. Assessing the Performance of the FAO AquaCrop Model to Estimate Maize Yields and Water Use under Full and Deficit Irrigation with Focus on Model Parameterization. *Agric. Water Manag.* **2014**, *144*, 81–97. [[CrossRef](#)]
79. Morris, M.D. Factorial Plans for Preliminary Computational Experiments. *Technometrics* **1991**, *33*, 161–174. [[CrossRef](#)]
80. Stott, L.D. The Influence of Diet on the $\delta^{13}\text{C}$ of Shell Carbon in the Pulmonate Snail *Helix Aspersa*. *Earth Planet. Sci. Lett.* **2002**, *195*, 249–259. [[CrossRef](#)]
81. Krause, P.; Boyle, D.P. Comparison of Different Efficiency Criteria for Hydrological Model Assessment. *Adv. Geosci.* **2005**, *5*, 89–97. [[CrossRef](#)]
82. Wellens, J.; Raes, D.; Tychon, B. On the Use of Decision-Support Tools for Improved Irrigation Management: AquaCrop-Based Applications. In *Current Perspective on Irrigation and Drainage*; INTECH: London, UK, 2017; pp. 53–67.
83. Zhuo, L.; Hoekstra, A. The Effect of Different Agricultural Management Practices on Irrigation Efficiency, Water Use Efficiency and Green and Blue Water Footprint. *Front. Agric. Sci. Eng.* **2017**, *4*, 185–194. [[CrossRef](#)]
84. Raes, D.; Steduto, P.; Hsiao, T.C.; Fereres, E. Calculation Procedures. In *AquaCrop-Reference Manual*; The Food and Agriculture Organization (FAO): Rome, Italy, 2017.
85. Raes, D.; Geerts, S.; Kipkorir, E.; Wellens, J.; Sahli, A. Simulation of Yield Decline as a Result of Water Stress with a Robust Soil Water Balance Model. *Agric. Water Manag.* **2006**, *81*, 335–357. [[CrossRef](#)]
86. Navarro-Hellín, H.; Martínez-del-Rincon, J.; Domingo-Miguel, R.; Soto-Valles, F.; Torres-Sánchez, R. A Decision Support System for Managing Irrigation in Agriculture. *Comput. Electron. Agric.* **2016**, *124*, 121–131. [[CrossRef](#)]
87. Raes, P.D.; Steduto, T.C.; Hsiao, E.F. *FAO Crop.-Water Productivity Model to Simulate Yield Response to Water. Reference Manual*; Food and Agriculture Organization of the United Nations: Rome, Italy, 2017.
88. Allen, R.G.; Pereira, L.S.; Raes, D.; Smith, M.; Ab, W. Crop Evapotranspiration-Guidelines for Computing Crop Water Requirements. In *FAO Irrigation and Drainage Paper 56*; Food and Agriculture Organization: Rome, Italy, 1998; pp. 1–15.
89. Lamn, F.; Ayars, J.; Nakayama, F. Irrigation Scheduling. In *Microirrigation for Crop Production*; Developments in Agricultural Engineering 13; Freddie, R., Lamm James, E., Ayars Francis, S., Nakayama, Eds.; Elsevier: Houston, TX, 2015; pp. 61–128.
90. Sutton, B.; Merit, N. Maintenance of Lettuce Root Zone at Field Capacity Gives Best Yields with Drip Irrigation. *Sci. Hortic. (Amsterdam)* **1993**, *56*, 1–11. [[CrossRef](#)]
91. Tan, S.; Wang, Q.; Zhang, J.; Chen, Y.; Shan, Y.; Xu, D. Performance of AquaCrop Model for Cotton Growth Simulation under Film-Mulched Drip Irrigation in Southern Xinjiang, China. *Agric. Water Manag.* **2018**, *196*, 99–113. [[CrossRef](#)]

92. Fazilah, W.; Ilahi, F.; Ahmad, D.; Husain, M.C. Effects of Root Zone Cooling on Butterhead Lettuce Grown in Tropical Conditions in a Coir-Perlite Mixture. *Hortic. Environ. Biotechnol.* **2017**, *58*, 1–4. [[CrossRef](#)]
93. Zhang, G.; Johkan, M.; Hohjo, M.; Tsukagoshi, S.; Maruo, T. Plant Growth and Photosynthesis Response to Low Potassium Conditions in Three Lettuce (*Lactuca sativa*) Types. *Hortic. J.* **2017**, *86*, 229–237. [[CrossRef](#)]
94. Dufault, R.J.; Ward, B.; Hassell, R.L. Dynamic Relationships between Field Temperatures and Romaine Lettuce Yield and Head Quality. *Sci. Hortic. (Amsterdam)* **2009**, *120*, 452–459. [[CrossRef](#)]
95. Parker, R.O. *Plant. & Soil Science: Fundamentals and Applications*, 1st ed.; Delmar Cengage Learning: Independence, KY, USA, 2009.
96. Wheeler, T.R.; Hadley, P.; Morison, J.I.; Ellis, R.H. Effects of Temperature on the Growth of Lettuce (*Lactuca sativa* L.) and the Implications for Assessing the Impacts of Potential Climate Change. *Eur. J. Agron.* **1993**, *2*, 305–311. [[CrossRef](#)]
97. Abdullah, K.; Ismail, T.G.; Yusuf, U.; Belgin, C. Effects of Mulch and Irrigation Water Amounts on Lettuce's Yield, Evapotranspiration, Transpiration and Soil Evaporation in Isparta Location, Turkey. *J. Biol. Sci.* **2004**, *4*, 751–755.
98. Gallardo, M.; Snyder, R.L.; Schulbach, K.; Jackson, L.E. Crop Growth and Water Use Model for Lettuce. *Irrig. Drain. Eng.* **1996**, *122*, 354–359. [[CrossRef](#)]
99. Boote, K.J.; Jones, J.W.; Pickering, N.B. Potential Uses and Limitations of Crop Models. *Agron. J.* **1996**, *88*, 704–716. [[CrossRef](#)]
100. Silvestro, P.C.; Pignatti, S.; Yang, H.; Yang, G.; Pascucci, S.; Castaldi, F.; Casa, R. Sensitivity Analysis of the Aquacrop and SAFYE Crop Models for the Assessment of Water Limited Winter Wheat Yield in Regional Scale Applications. *PLoS ONE* **2017**, *12*, 1–30. [[CrossRef](#)] [[PubMed](#)]
101. Wallach, D.; Keussayan, N.; Brun, F.; Lacroix, B.; Bergez, J. Assessing the Uncertainty When Using a Model to Compare Irrigation Strategies. *Agron. J.* **2008**, *104*, 1274–1283. [[CrossRef](#)]



© 2018 by the authors. Licensee MDPI, Basel, Switzerland. This article is an open access article distributed under the terms and conditions of the Creative Commons Attribution (CC BY) license (<http://creativecommons.org/licenses/by/4.0/>).